NEES/E-Defense Tests: Seismic Performance of Ceiling / Sprinkler Piping Nonstructural Systems in Base Isolated and Fixed Base Building

S. Soroushian, K. L. Ryan, M. Maragakis, & J. Wieser
University of Nevada, Reno

T. Sasaki & E. Sato
National Research Institute for Earth Science and Disaster Prevention

T. Okazaki
Hokkaido University

L. Tedesco
USG Building Systems

A. E. Zaghi
University of Connecticut

G. Mosqueda
State University of New York at Buffalo

D. Alvarez
CISCA

SUMMARY:
Recent earthquakes have conclusively demonstrated that nonstructural damage results in significant loss of property and function with major catastrophic impact on communities. As part of the NEESR-GC project and in a collaborative effort with NEES TIPS and NIED, a full-scale, five-story steel moment frame building in base-isolated and fixed-base configurations was subjected to a number of 2D and 3D ground motions using the E-Defense shake table. The building was tested under three different configurations: 1) base isolated with triple pendulum bearings (TPB), 2) base isolated with a combination of lead-rubber bearings and cross linear bearings (LRB/CLB), and 3) fixed base. For this experiment, more than 800 sq-ft of suspended ceiling with lay-in tiles and 3 sprinkler branch lines were installed on the 4th and 5th floors of the building. This paper presents some of the preliminary observations related to the response of nonstructural systems from these experiments.

Keywords: Nonstructural Systems, Base Isolation, Experimental

1. INTRODUCTION

This is one of four papers reporting a collaborative program on base-isolated buildings conducted under the Memorandum of Understanding between the National Institute of Earth Science and Disaster Prevention (NIED) of Japan and the National Science Foundation (NSF), George Brown Jr. Network for Earthquake Engineering Simulation (NEES) program of the U.S. As part of these full scale shake table tests performed at E-Defense, the "NEESR-GC: Simulation of the Seismic Performance of Nonstructural System" was commissioned to augment the building with an integrated partition-ceiling-sprinkler piping system on the upper stories.

The total repair and replacement cost of nonresidential buildings after the Northridge earthquake was $6.3 billion, only $1.1 billion of which was due to structural damage (Kircher 2003). Immediately after this earthquake, 88% of the occupants of hospital beds in the damaged area (13 hospitals) were evacuated as a result of water damage, elevator failure, and other nonstructural damage (Ayres et al. 1998). Minimal structural damage was observed in hospitals that met the requirements specified in the 1973 Hospital Act. Nevertheless, even in hospitals constructed after 1973, and which survived strong

ground motions, nonstructural damage of the plumbing, ceiling systems, etc., was extensive. This demonstrates an urgent need to better understand the seismic behavior of nonstructural systems.

The nonstructural design provisions cannot be improved without strategically collected experimental data that supplement field observation. Several studies have been conducted on the seismic response of nonstructural subassemblies and their components, such as ceiling tiles and piping systems, as early as the 1980s (ATC 2007). Our understanding of the system-level response of nonstructural systems remains very limited, and could be improved substantially by large-scale experiments on complete systems (Zaghi et al. 2012).

This paper reports on the response of the ceiling and fire sprinkler piping systems, which were installed in a full-scale building tested in three different configurations: 1) base isolated with triple pendulum bearings (TPB), 2) base isolated with a combination of lead-rubber bearings and cross linear bearings (LRB/CLB), and 3) base fixed.

2. TEST BUILDING

Nonstructural elements were installed in a 5-story steel moment frame building (Fig. 1) that was tested for the NEES TIPS/E-Defense project. This building is approximately 16 m (53 ft) tall, and asymmetric in plan with dimension of 10 m (33 ft) by 12 m (40 ft) (2 bays by 2 bays) (Fig. 2). Further information about the building is provided in Kasai et al. (2010).

The building weighed about 5,300 kN. The dynamic properties of the building measured and reported from previous tests are: natural period = 0.68 sec, damping ratio = 2%. The modeling and analysis of the building specimen for 2011 experiments will be reported in future papers; preliminary results suggest the specimen in the fixed-base configuration may have responded with slightly longer period and greater damping ratio than in previous tests.

Figure 1. 5-story steel moment frame specimen set on triple pendulum isolators

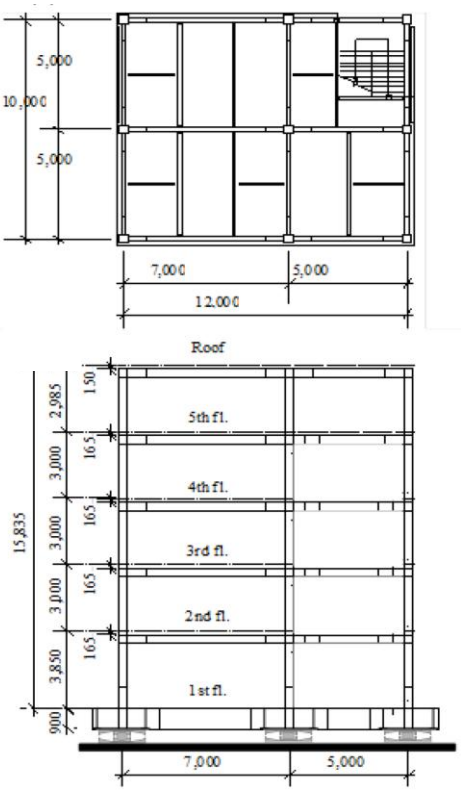

Figure 2. Top: plan view, bot.: elevation view

T

wo isolation systems were considered and designed in addition to the fixed base configuration in this experiment. The first isolation system incorporated 9 identical TPBs, one beneath each column, which were manufactured by Earthquake Protection Systems. The second isolation system incorporated 4 LRBs manufactured by Dynamic Isolation Systems and 5 CLBs manufactured by THK according to design specified by Aseismic Devices Company (ADC). Additional details of the isolation design are provided in (Ryan et al. 2012).

3. NONSTRUCTURAL SYSTEMS

A partition-ceiling-sprinkler piping subassembly was designed and installed in nearly identical configuration over two complete floors of the building specimen. These components were installed on the 4th and 5th floors, which were expected to draw the maximum floor accelerations.

3.1. Suspended Ceiling

The layout of the ceiling system for each floor is shown in Fig. 3, along with a photograph of the grid system prior to the panel installation. The ceilings were installed in the test frame per ASTM E580/E580M-11ae1 (ASTM 2011). The grid was constructed using the heavy-duty USG DONN 23.8 mm (15/16 in) exposed tee system. Main runners and cross tees were aligned as shown in Fig. 3(a). The main runners were hung with 12-gauge Hilti X-CW suspension wires spaced 1.2 m (4 ft) apart; additional wires supporting all perimeter grid pieces were placed within 200 mm (8 in) from the face of the partition wall. The ceiling was suspended 1 m (3 ft) from the bottom of the structural deck.

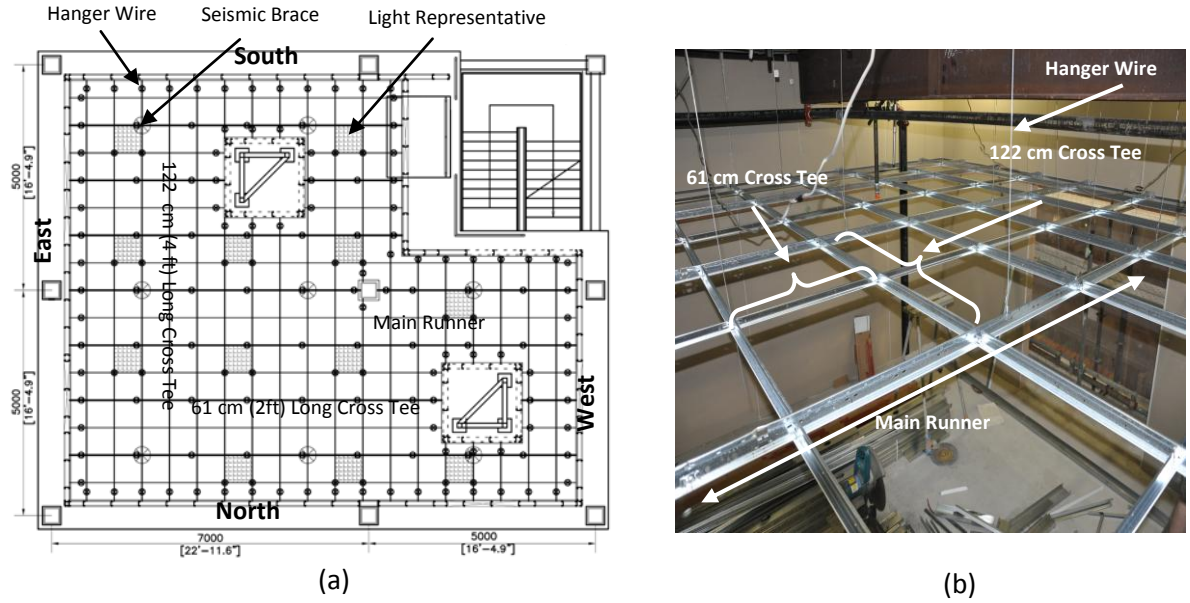

Figure 3. Overall view of ceiling system; (a) layout; and (b) photograph of grid prior to panel installation

A 22 mm (7/8 in) wall molding was attached to the perimeter partition walls. At the North and East ends, the main runners and cross tees were attached tight to the wall molding using USG/ACM7 seismic clips with one partition attached screw and one top hole screw to prevent movement of ceiling grids (Fig. 4(a)). At the South and West ends, the main runners and cross tees were attached with 19 mm (3/4 in) clearance to the wall molding using the same seismic clip, but with the second screw attached at the middle of the clip slot to allow the grid members to float freely (Fig. 4(b)). At the hatched grids in Fig. 3(a), heavier gypsum board panels were used to represent the weight of light fixtures.

ASTM E580/E580M-11ae1 (ASTM 2011) require seismic braces to be placed in ceiling areas larger

than 93 m2 (1,000 ft2). To compare the behavior of braced and unbraced ceiling systems, the seismic braces were only installed on the 5th floor ceiling while all other details were identical on both floors. Each seismic brace consisted of: 1) a system of splay wires or a rigid brace and 2) a USG/VSA30/40 compression post. The seismic braces were placed at 3.6 m (12 ft) on center, in each direction, with the first set occurring within 1.8 m (6 ft) of the face of the wall. Four wires splayed at 90° from each other were attached to the main runner within 50 mm (2 in) of an intersection with cross members (Fig. 5). In some locations, due to the geometry and connection constraints, steel stud compression posts were used instead of USG/VSA30/40 compression posts and/or 2 way steel stud rigid braces were used in place of two of the splay wires.

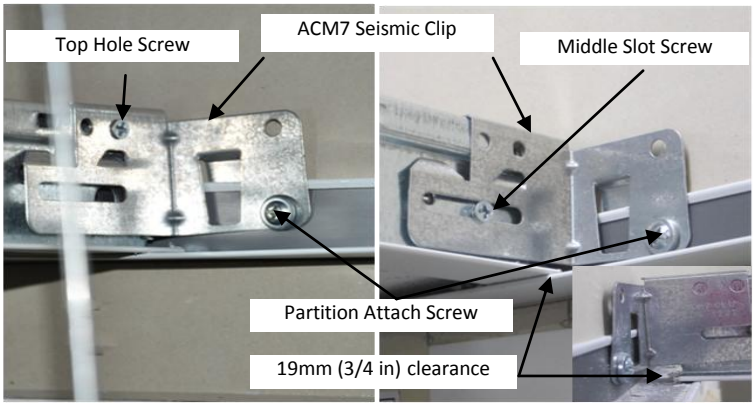

Figure 4. Joint between runners/cross tees and wall molding: (a) attached Detail, and (b) unattached detail (free to float)

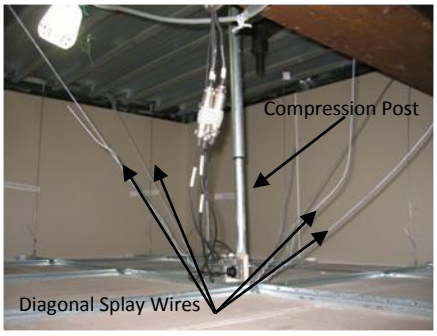

Figure 5. Seismic bracing for the ceiling grid

3.2 Fire Sprinkler Piping

A standard Schedule 40 piping system was attached to the specimen per NFPA 13 (NFPA 2011). The piping system included one 80 mm (3 in) diameter riser pipe, one 65 mm (2.5 in) diameter main run and three (North-South) 32-25 mm (1.25-1 in) diameter branch lines (Fig. 6).

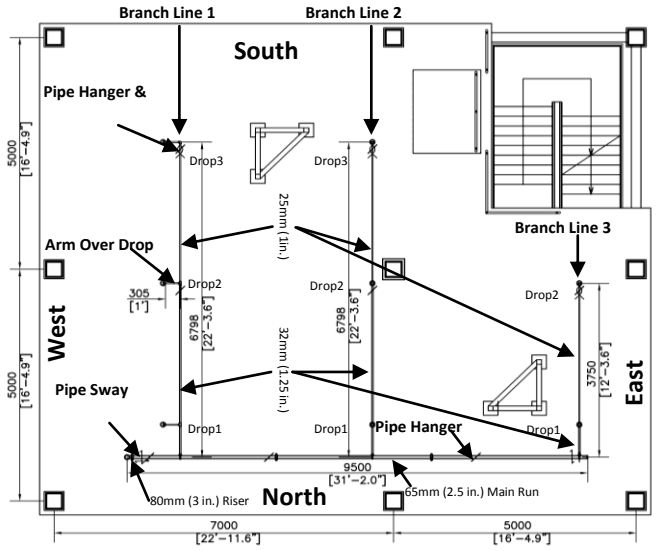

Figure 6. Overall plan view of piping system

All connections on the riser, the main run, and branch line to the main run intersections were grooved fit, while the rest of the connections were threaded. Branch Lines 1 and 2, each with three 305 mm (12 in) drops, incorporated armover drops and straight drops, respectively. At the first drop of each branch

line, a 50 mm (2 in) oversized ring was used at the location of the sprinkler heads (oversized gap configuration, Fig. 7(a)), while only minimal gap was provided for the rest of drops (no gap configuration, Fig. 7(b)). A Victaulic Aquaflex Flexible drop was used at Drop 2 of Branch Line 3 (Fig. 7(c)).

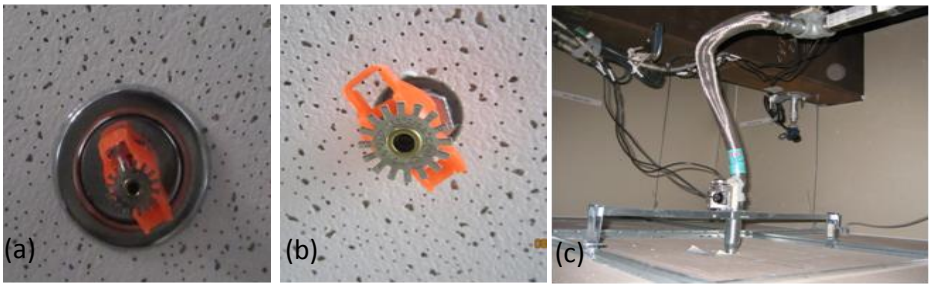

Figure 7. Sprinkler heads and drops: (a) 50 mm (2 in.) oversized gap configuration, (b) no gap configuration, and (c) flexible drop

On each floor, the piping system was supported by vertical pipe hangers at 9 locations, 4 for the main run and 5 for the branch lines (Fig. 8(a)). The pipe hangers consisted of 9.5 mm (3/8 in) diameter and 457 mm (1.5 ft) long threaded rod. Lateral resistance was provided by inclined 25 mm (1 in) diameter longitudinal and lateral pipe sway braces on the main run near the riser pipe (Fig. 8(b)), a lateral pipe sway brace at the end of the main run, and two longitudinal braces at the end of the riser pipe below the 4th floor deck. The ends of the branch lines were restrained with two diagonal splay wires to limit the lateral movement (Fig. 8(a)).

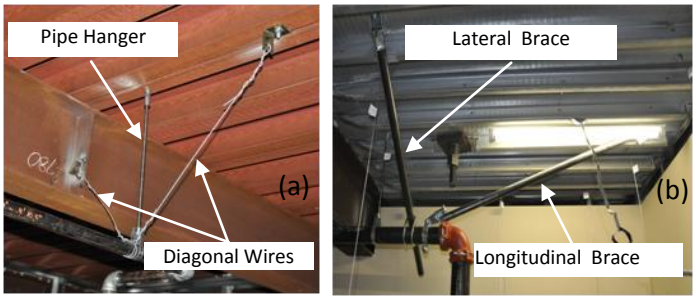

Figure 8. Bracing for piping system: (a) diagonal Splay wires and pipe hanger at the end of each branch line, and (b) lateral and longitudinal brace near riser

4. EXPERIMENTAL RESULTS

The building was subjected to a variety of horizontal (2D) and combined horizontal and vertical (3D) ground motions. The applied ground motions are summarized in Ryan et al. (2012). Due to the flexibility of the decks, the vertical acceleration was generally amplified in the middle of the decks compared to the column locations. Also, the North-East and South-East side of the roof deck experienced the largest vertical acceleration due to supplementary roof-mounted mass (Ryan et al. 2012). The vertical natural frequency of the 5th and 6th decks are provided in Soroushian et al. (2012).

While almost no damage to the ceiling-piping system was observed in response to 2D (horizontal only) ground excitations, significant damage was observed from 3D motions with large vertical ground excitation. The greatest damage was generated by a 3D input ground motion recorded at Rinaldi Receiving Station during the 1994 Northridge Earthquake (3D-Northridge-Rinaldi) that was repeated in all three system configurations. (Note that the scale factor for the horizontal component of

excitation was reduced for the fixed-base building.) Although minor differences were observed, the damage mechanisms and the extent of damage (e.g. affected area) were very similar for the three system configurations. Although the ceiling-piping system was repaired after each test day, it was never restored to its original configuration. Thus, unless otherwise noted, all observations reported here are from the first test that triggered damage – 3D-Northridge-Rinaldi in TPB isolated building.

4.1 Ceiling Panel and Grid System Failures

During the experiments, a maximum of three panels (1%) from the unbraced (4th floor) ceiling were displaced or fell to the floor in while up to 40% of the panels in the braced (5th floor) ceiling were displaced and/or fell. Most of the damage was located under the North-East and South-East decks. The condition of the braced and unbraced ceiling after 3D-Northridge-Rinaldi (TPB system) is compared in Fig. 9. Over the course of the test program, some of the cross tee sections failed but the main runners always remained intact.

Figure 9. Condition of (a) braced ceiling (5th floor) and (b) unbraced ceiling (4th floor) after 3D-Northridge-Rinaldi (TPB system)

The accelerations in all three directions at the deck level, which represent the input excitation to the ceiling system, were slightly higher at the 6th deck than the 5th deck. However, the input acceleration alone does not explain the difference in damage; observed accelerations in each ceiling suggest that the compression posts used in the lateral bracing increased the damage to the ceiling system in this experiment. Fig. 10 shows the vertical acceleration of a ceiling panel and ceiling grid measured for a moderate excitation (3D-Superstition Hills Westmorland/TPB system) executed prior to the occurrence of ceiling damage. In the unbraced ceiling, little amplification of the panel acceleration relative to the grid was observed (Fig. 10(a)), which suggests that these two components moved together. However, in the braced system, the acceleration of the ceiling panel is significantly amplified relative to the compression post attachment location (Fig.10(b)), which suggests that the panel pounded on the grid system.

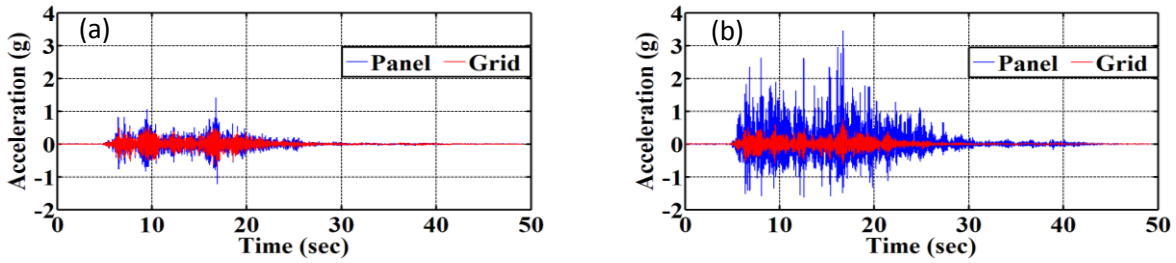

Figure 10. Vertical acceleration in panel versus grid in (a) 4th floor (unbraced) and (b) 5th floor (braced) ceiling due to 3D-Superstition Hills – Westmorland (TPB system)

The acceleration trends observed in Fig. 10 are explained as follows: consider the diagram of the ceiling system in Figures 11 and 12, where the vertical acceleration of the deck, grid, and panel are

labeled A_{deck}, A_{grid}, and A_{panel}, respectively. Fig. 11 depicts the unbraced ceiling, which is supported only by hanger wires. When the hanger wires are in tension (case 1), the accelerations of the deck, grid and panel are the same. However, when the hanger wires are loose (case 2), which as an example can be initiated by downward deck acceleration of more than 1g while the panels and grid system are limited to a maximum of 1g downward acceleration, the deck acceleration will differ from that of the panels and grid system. As the panel and grid system have almost the same acceleration, the panels will remain in place between the grid members and the probability of dislodging panels is low. Fig. 12 depicts the braced ceiling with compression posts at regular intervals. By constraint of the compression posts, the entire system (deck, grid, and panels) will generally move together with equal accelerations, as depicted in case 1. However, during downward deck acceleration of more than 1g, the grid system will move with the deck (assuming the compression posts are rigid) at the compression post locations while the panels are limited to 1g downward acceleration. As a result, the deck and grid accelerations will differ from the panel accelerations, causing a gap to form between the ceiling grid and panels. Once the gap forms, the ceiling panels are no longer constrained by the horizontal forces of the grid system, and hence the panels will "pop out" of the grid. Furthermore, the ceiling panels will impact the grid system when they fall, weakening the grid members.

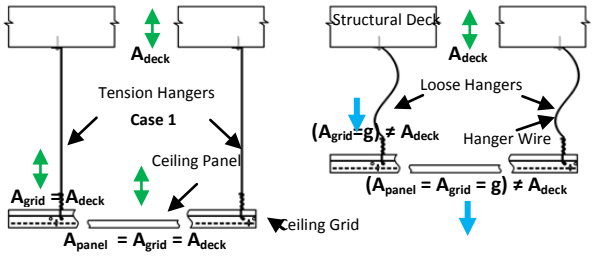

Figure 11. Vertical dynamics of unbraced ceiling

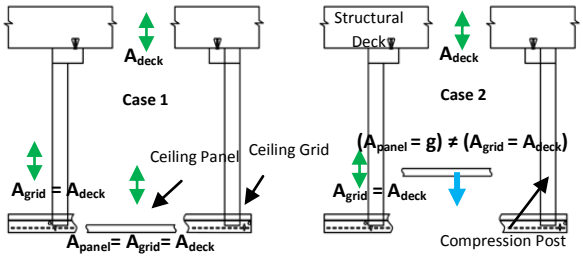

Figure 12. Vertical dynamics of braced Ceiling

4.2 Ceiling Perimeter Attachment Damage

Fig. 13 shows minor damage observed at the unattached joints between grid members and wall molding. The mechanism is interpreted as follows: when the grid member moved away from the wall, the grid member lost contact with the wall molding (Fig. 14(a)). Since the middle slot is large relative to the screw dimensions, the grid member may settle slightly (Fig. 14(b)). As the settled grid member moved back toward the wall, it hit the wall molding to cause the observed damage (Fig. 14(c)). Note that ASTM E580/E580M-11ae1 (ASTM 2011) permits the use of either 22-mm (7/8-in.) or 50-mm (2-in.) wall molding to support seismic clips, and therefore, by installing the grid members with 19mm (3/4-in.) clearance from the wall, only 3.2mm (1/8-in.) seat length will be available from the edge of wall angle.

Figure 13. Ceiling perimeter attachment failure after 3D-Northridge-Rinaldi (TPB system)

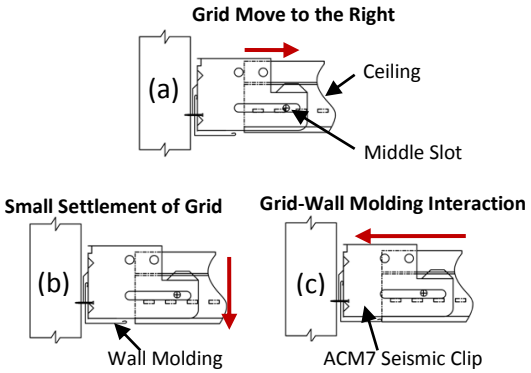

Figure 14. Grid - wall molding interaction mechanism

Based on the data from the experiment, fragility curves were developed to represent the statistical likelihood of occurrence of the ceiling perimeter damage shown in Fig. 13. These fragility curves are

shown in Fig. 15, and represent the probability that the ceiling movement relative to the partition walls on the unattached side (D_{cp}) exceeds 3.2 mm (1/8 in) -which would likely cause unseating- as a function of peak floor acceleration (PFA). The plots in Fig. 15 are represented by the following lognormal cumulative distribution function (Nielson and DesRoches, 2007):

$$P(EDP \geq EDP_o \mid IM) = \Phi\left(\frac{\ln(a) + b\ln(IM) - \ln(EDP_o)}{\beta d / IM}\right) \tag{4.1}$$

where a and b are regression coefficient and EDP_o is the limit state for ceiling relative movement. In this equation, $\beta_{d/IM}$ is the dispersion and $\Phi[\cdot]$ is the cumulative normal distribution function).

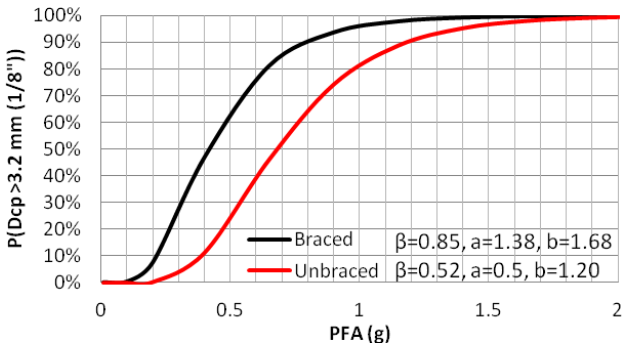

Figure 15. Probability of grid-wall angle interaction

Fig. 15 shows that at PFA of 1(g) the probability of unseating was more that 80% in all cases. Unseating could perhaps be avoided by increasing the seat length of the 22 mm (7/8 in) wall molding.

4.3 Permanent Rotation of Armover Drops

A vulnerability of armover drops compared to straight drops was observed in these experiments. During 3D-Northridge-Rinaldi (TPB system), the entire 5th floor Branch Line 1 with three armover drop pipes twisted around its connection point to the main run (Fig. 16(a)). Due to vertical acceleration, a vertical inertia force is generated proportional to the mass of the armover drop. The twisting moment around the branch line is the summation of the torque generated at each drop (Fig. 16(b)). The current code (NFPA 2011) permits the connections along this branch line to be designed without torsional resistance since the cumulative horizontal length of the unsupported armover less than 610 mm (24 in). However, the torsional resistance of the threaded joints was not sufficient to resist the cumulative torsional demand generated in the large vertical excitation, and permanent twisting of the branch line was observed.

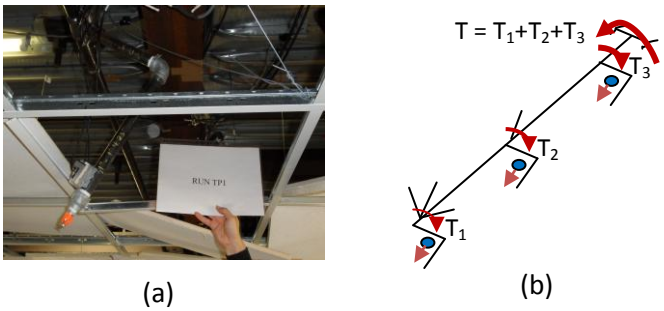

Figure 16. (a) Armover permanent rotation after 3D-Northridge–Rinaldi (TPB system), and (b) torsional demand on armover branch line

4.4 Damage Near Sprinkler Heads

Wherever rigid drop pipes were used, the sprinkler head damaged the ceiling panels regardless of whether the oversized gap configuration, which conforms to code requirements (ASTM, 2011), or the no gap configuration were used. Pounding of the sprinkler heads against the ceiling panels produced damage to the ceiling panels even in motions with moderate horizontal floor accelerations. As an extreme example, a 200 mm (8 in) long piece was knocked out of the ceiling panel during (2D - Tohoku- Iwanuma/base fixed) (Fig. 17(a)), which is much larger than the 50 mm (2 in) gap required by code. On the other hand, no damage was observed around the flexible hose fittings that were mounted at the end of Branch Line 3 (Fig. 17(b)).

Figure 17. Comparison of observed damage near (a) conventional sprinkler head, and (b) flexible hose sprinkler head after 2D-Tohoku-Iwanuma (base fixed)

4.5 Failure of the Pipe Hangers

Another response mode that was clearly observed during testing was formation of a gap between the pipe and the hanger ring of the pipe hanger. The vibration and subsequent pounding of the pipe against the hanger ring led to failure of the hanger ring connection (Fig. 18). This behavior is probable in large vertical excitation, where the pipe hanger threaded rod has not been detailed to extend down to the pipe. Fig. 19 depicts this failure that was observed at two hangers near the riser pipe on both floors.

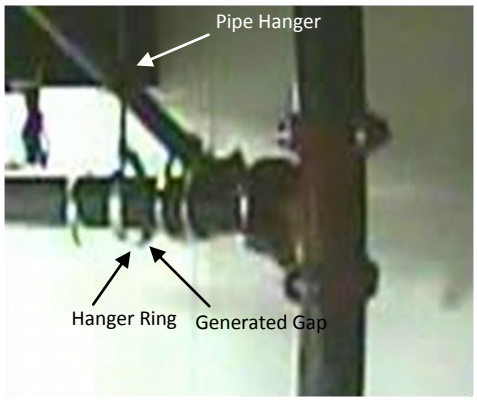

Figure 18. Captured frame from recorded video that shows the generated gap Between Pipe and hanger ring during 3D-Northridge–Rinaldi (TPB System)

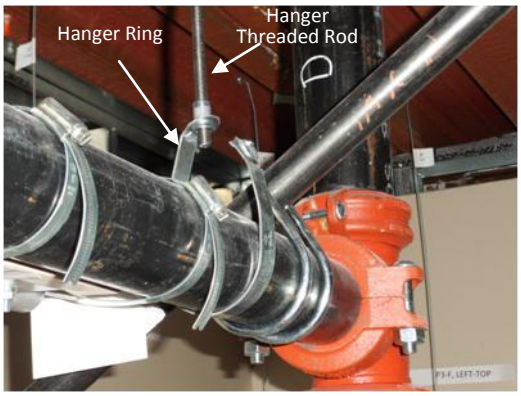

Figure 19. Pipe hanger ring failure after 3D-Northridge–Rinaldi (TPB System)

5. SUMMARY OF OBSERVATIONS

The major observations of this experiment are summarized below.

- Use of lateral bracing including compression posts may not improve the seismic response of

ceiling, especially if the system is subjected to strong vertical excitation.

- Due to the twisting moment generated from the armover drops, long branch line pipes with several unsupported armover drops are expected to twist around the branch line threaded connection point.
- The oversized gap configuration with 50 mm (2 in) ring was not effective to prevent damage to ceiling panels resulting from sprinkler head pounding; however, the use of flexible hose drops substantially reduced the piping-ceiling interaction.
- The pounding of the pipe against the hanger ring in vertical excitation led to failure of the hanger ring connection.
- These observed response mechanisms may be sensitive to specific circumstances of the experiments, such as building configuration (e.g. slab vibration characteristics) and acceleration demands (e.g. large vertical acceleration relative to horizontal acceleration).

6. ACKNOWLEDGEMENTS

This material is based upon work supported by the National Science Foundation under Grant No. 0721399. This GC project to study the seismic response of nonstructural systems is under the direction of M. Maragakis from the University of Nevada, Reno and Co-PIs: T. Hutchinson (UCSD), A. Filiatrault (UB), S. French (G. Tech), and B. Reitherman (CUREE). Any opinions, findings, conclusions or recommendations expressed in this document are those of the investigators and do not necessarily reflect the views of the sponsors. The input provided by the Practice Committee of the NEES Nonstructural Project, composed of W. Holmes (Chair), D. Allen, D. Alvarez, and R. Fleming; by the Advisory Board, composed of R. Bachman (Chair), S. Eder, R. Kirchner, E. Miranda, W. Petak, S. Rose and C. Tokas, has been crucial for the completion of this research. The authors recognize and thank the following companies for providing product donations and technical support: USG Building systems, Victaulic, Tolco, Hilti, CEMCO steel, and Allan Automatic Sprinkler.

REFERENCES

ASTM E580/E580M-11ae1. (2011). "Standard Practice for Installation of Ceiling Suspension Systems for Acoustical Tile and Lay-in Panels in Areas Subject to Earthquake Ground Motions." *ASTM International*, Volume **04**.06.

ATC. (2007). FEMA 461-Interim protocols for determining seismic performance characteristics of structural and nonstructural components through laboratory testing. Redwood City, CA.

Ayres, J.M., Phillips, R.J. (1998)."Water Damage in Hospitals Resulting from the Northridge Earthquake." *ASHRAE Trans*., Vol. 104, Part 1, American Society of Heating, Refrigerating and Air-Conditioning Engineers, Atlanta, Georgia.

Kircher, C. A. (2003). "It Makes Dollars and Sense to Improve Nonstructural System Performance." *ATC-29-2 Proceedings of Seminar on Seismic Design, Performance, and Retrofit of Nonstructural Components in Critical Facilities.*

Kasai, K., et al. (2010). "Full scale shake table tests of 5-story steel building with various dampers." Proc., *7th Intern. Conf. on Urban Earthquake Engin. & 5th Intern. Conf. on Earthquake Engin*. Tokyo Inst. Tech., Tokyo, Japan.

NFPA13. (2011). "Standard for the Installation of Sprinkler Systems." *National Fire Protection Association*, 2010 Edition, Quincy, MA.

Nielson, G. B. and DesRoches, R., (2007) Analytical Seismic Fragility Curves for Typical Bridges in the Central and Southeastern United States, Earthquake Spectra, EERI, 23(3), Oakland, CA, 615-633.

Ryan, K., Dao, N, Sato, E., Sasaki, T., and Okazaki, T. (2012) "Aspects of Isolation Device Behavior Observed from Full-Scale Testing of an Isolated Building at E-Defense." *43rd Structures Congress*, ASCE, Chicago, USA.

Soroushian, S., et al., (2012) "Seismic Response of Ceiling/Sprinkler Piping Nonstructural Systems in NEES TIPS/NEES Nonstructural/NIED Collaborative Tests on a Full Scale 5-Story Building" *43rd Structures Congress*, ASCE, Chicago, USA.

Zaghi, A. E., Maragakis, E. M., Itani, A., and Goodwin, E. (2012). "Experimental and Analytical Studies of Hospital Piping Subassemblies Subjected to Seismic Loading." *Earthquake Spectra, EERI*. **26**(1), EERI